ANALYSIS OF THE OPTICAL ABSORPTION AND PHOTOINDUCED BIREFRINGENCE IN As_2S_3 CHALCOGENIDE FILMS

Mihai STAFE[1], Georgiana C. VASILE[1], Constantin NEGUȚU[1], Aurelian A. POPESCU[2,] Laurentiu BASCHIR[2], Mona MIHĂILESCU[1], Niculae N. PUŞCAŞ[1]

In this paper we report several theoretical and experimental results concerning the characterization of As_2S_3 film chalcogenide glasses by photoinduced optical absorption. We evaluated the absorption coefficient of the chalcogenide glasses using Tauc model in the range 450 nm÷510 nm and the Urbach energy.

The photoinduced birefringence of the chalcogenic film is analyzed experimentally by using a CW pump laser at 520 nm wavelength. At the pump laser intensity of 100 mW/cm^2, the transmission of the probe beam at the same wavelength increases approximately linearly during the first 90 minutes and saturates at later times. This is connected to the small film absorption at the pump wavelength, and to the destructive interference of the probe beam by multiple reflections within the chalcogenic film which enhances the film transmission during the pump irradiation.

The above mentioned theoretical and experimental results may be used for the fabrication of the amorphous As_2S_3 chalcogenide film glasses and also for the better understanding of the absorption mechanisms in these structures.

Keywords: plasmonics, photonics, As_2S_3 thin surface films, photoinduced optical absorption

1. Introduction

After the discovery of surface plasmons [1]-[3] several papers have been published in the last years concerning theoretical explanations and experimental characterization [3]-[7] of the surface plasmon resonance in multilayer structures including chalcogenide thin films. Plasmonic nanostructures consisting of tens of nanometer thick metallic layers and hundreds of nanometer thick chalcogenide films have attracted significant interest due to their unique chemical and physical properties and potential applications in: enhancement of Raman scattering, catalysis, sensing, nanofabrication for the next generation of electronic devices, photoluminescence, bio-light emission devices, and solar cells. Also, another

[1], Physics Department, University POLITEHNICA of Bucharest, Splaiul Independentei, 313, 060042, Bucharest, Romania
[2] National Institute R&D of Optoelectronics, INOE 2000, 409 Atomistilor str., PO BOX MG. 5, 77125 Magurele, Ilfov, Romania
Corresponding author: Georgiana C. Vasile: georgiana.vasile@physics.pub.ro

interesting application could be the development of all-optical memory using photo-induced optical transmission that occurs in films of semiconductor chalcogenide glasses after the irradiation with polarized light. Low loss planar waveguides can be realized using a multilayer structure of As_xS_{1-x} chalcogenide films with different compositions.

In the last years the photoinduced phenomena in chalcogenide thin film glasses attracted the attention of physicists and engineers because they produce structural transformations and photoinduced optical anisotropy [8]-[14]. Photoinduced structural transformations and defects (e.g. color centers) result in reversible effects of photodarkening due to the change of the optical band gap, film transparency and also in the change of some other film properties such as the change of solubility in different organic and inorganic solvents.

Photoinduced optical anisotropy is the emergence of dichroism and/or birefringence in an initially optically isotropic chalcogenide film under the action of linearly polarized light. This effect is explained by the orientation of interatomic bonds or specific defects of the glass, leading to the appearance of some optical axis with a direction determined by the polarization vector of the exciting light. Chalcogenide glasses display the highest photoinduced effects among other materials, their photosensitivity does not involve chemical reactions.

In spite of the long history of experimental and theoretical studies, there are still no well-accepted models for photoinduced changes in chalcogenide glasses. These effects, photodarkening and photoinduced anisotropy in chalcogenide glassy films, are intensively studied for their applications in electro-optics.

The change of the optical transmission in As_2S_3 films are preserved after the pump irradiation is finished, unlike the bulk compounds As_2S_3, where the optical transmission is restored after the cessation of the illumination [3]. This effect may be used for the fabrication of a 2D optical memory cell. The higher the pump beam intensity, the faster changes of the optical transmission may be obtained.

Here we analyze theoretically and experimentally the optical properties of As_2S_3 thin films deposited by thermal vacuum evaporation in the spectral domain in the vicinity of the absorption edge. The article has the following structure: Section 2 presents the fabrication method of the As_2S_3 chalcogenide films, Section 3 is devoted to the theoretical considerations on optical absorption of chalcogenide films, Section 4 presents the experimental set-up for analyzing the optically induced birefringence while in Section 5 we discuss the theoretical and experimental results of our study concerning the optical properties of the chalcogenide thin films. Finally, in Section 6 we present our conclusions concerning the obtained results.

2. Fabrication of As_2S_3 thin films

Nanostructures (for instance multilayer structure chalcogenide films) 15 nm thick have attracted significant interest due to their unique chemical and physical properties and potential applications in: sensing, nanofabrication for the next generation of electronic devices, photoluminescence, bio-light emission devices and solar cells.

The optical properties of thin films are not always the same as those of corresponding bulk glasses, thus many techniques have been proposed to prepare thin films of chalcogenide glasses.

Pulsed laser deposition, RF sputtering on the films are well established deposition methods that maintain the stoichiometry of multi-element amorphous chalcogenide compounds [5], [6].

Thermal vacuum evaporation remains one of the basic deposition methods for materials which do not exhibit decomposition and whose evaporation temperature isn't too high. Low loss planar waveguides were obtained with amorphous As_2S_3 thin films prepared by RF sputtering [6]. As_2S_3 may be deposited by thermal evaporation and is one of the promising materials for plasmonic applications.

For the beginning, bulk chalcogenide glasses were synthesized using high purity elements As and S (of 6N) in quartz ampoules. Precursor elements were loaded in the ampoule, then the ampoule was evacuated and flame soldered. The temperature was raised slowly to the melting temperature of 870-920 °C. The maximum temperature of the liquid melt mixture was maintained for 24 hours along with the rotation about its axis and vibration in order to obtain a homogeneous mass. Next, the ampoule was cooled suddenly by taking it out of the furnace. Some of the synthesized chalcogenide glasses were cut into square parallel plates with dimensions 10x10x4 mm^3 and polished until they achieved a glossy surface suitable for optical measurements. A diamond disk was used as cutting tool.

Thin films were obtained by thermal evaporation of granular materials on microscope slide glasses in vacuum ($5 \cdot 10^{-6}$ Torr). Vacuum thermal evaporation is based on the formation of atomic and molecular flows by heating the source material. The flows travel without collisions from the evaporator to the substrate, where the material condenses to form a thin layer. Shape and reciprocal location of the source and substrate determine the thickness distribution. To obtain high quality thin films a special evaporator was developed, which uses indirect heating. Transparent amorphous films were obtained in the 125 ÷ 500 nm thickness domain on glass substrates.

3. Theoretical considerations on optical absorption

It was shown that in chalcogenide glasses the absorption edge is broader than in crystalline analogues and this is caused by a broad energy distribution of electronic states in the band gap due to disorder and defects. Based on the theoretical models presented in papers [8]-[14] the absorption coefficient of the chalcogenide glasses is given by the equation (Tauc model):

$$\alpha = \frac{B}{h\nu}\left(h\nu - E_g\right)^2 \tag{1}$$

where h is the Planck's constant, ν is the frequency, E_g represents the optical band gap, and B is a constant (Tauc parameter, respectively).

Eq. (1) is valid for a number of amorphous materials in the domain $10^4 cm^{-1} < \alpha < 10^5 cm^{-1}$ (i.e., Tauc region).

The parameter E_g corresponds to the energy difference between the onsets of exponential tails of the allowed conduction bands. For amorphous As_2S_3 the value of band gap was found to be =2.35÷2.4 eV.

The constant B includes information on the convolution of the valence band and conduction band states and on the matrix element of optical transitions, which reflects not only the relaxed k selection rule but also the disorder induced spatial correlation of optical transitions between the valence band and conduction band. Moreover, B is highly dependent on the character of the bonding. At the energy levels where the Tauc model is used the joint density of states does not include tail states. The information at the band tails may be obtained from the Urbach energy which is determined by the degree of disorder [8]-[14]. The parameter B is sensitive to topological disorder only when electronic structural changes occur and depends on the product of the oscillator strength of the optical transition, the deformation potential, and the mean deviation of the atomic coordinates.

Based on the theoretical model presented in paper [13] the constant B is given by:

$$B \propto \frac{\left[N(E_c)\right]^2}{n_o \Delta E_c} \tag{2}$$

where $N(E_c)$ is the density of states at the conduction band edge, n_o is the index of refraction, and ΔE_c corresponds to the width of the conduction band tail, respectively.

In the exponential part of the absorption edge where $\alpha < 10^4 cm^{-1}$ the absorption coefficient is governed by the Urbach rule [11]:

$$\alpha(h\nu) = \alpha_o \exp\left(\frac{h\nu}{E_e}\right) \tag{3}$$

where the Urbach energy, E_e characterizes the slope of this region. From the plot of the $\log(\alpha)$ on the photon energy one obtains a straight line. The calculated value of E_e is the inverse of the slope of the straight line and gives the width of the tails of the localized states into the gap at band edges. The Urbach edge is a useful parameter to evaluate the degree of disorder that of the chalcogenides is not very clear [13], [14].

4. Experimental setup for study of the optically induced birefringence

The experimental setup employed for analysis of the optically induced birefringence of a 240 nm thick As_2S_3 chalcogenide film deposited on a glass substrate is presented in Fig. 1. The linearly polarised laser beam from a Thorlabs MCLS diode laser system is divided by a beam-splitter, the transmitted and reflected beam being directed on the same area of the chalcogenide target as probe and pump beams, respectively. The 520 nm wavelength of the pump laser is near the absorption edge of the chalcogenide film, as is estimated from the Tauc plot in the next Section.

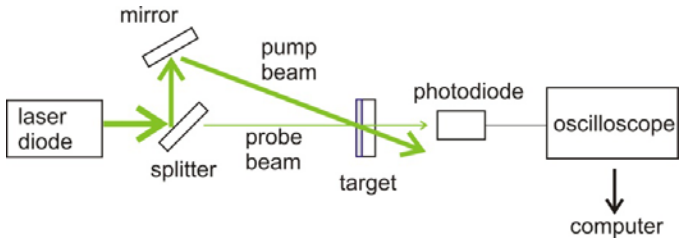

Fig.1. Experimental setup for optical characterization of As_2S_3 film chalcogenide film.

The probe beam passes at normal incidence through the chalcogenide target whereas the pump beam has an incidence angle of ~15 degrees. The probe beam has a much smaller power (~0.02 mW) as compare to the pump beam (2 mW), the intensity of the pump beam at the target surface being ~100 mW/cm^2. Thus, the modifications of the optical properties of the chalcogenide film are mainly influenced by the deposited energy of the pump beam.

The time variation of the film transmission for the probe beam is analysed by a rapid photodiode connected to an oscilloscope. The initial transmission of the film is determined to be ~65%. The average photo-signal from the oscilloscope is monitored every minute for ~140 min. Further analysis of the data on a computer

enabled us to evaluate the photo-induced birefringence of the chalcogenide film during the laser irradiation with the pump beam.

5. Discussion of the theoretical and experimental results

First, we determined by SEM and AFM methods the characteristics of the As_2S_3 surface films at nanometric scale. We used a FEI Quanta Ispect F scanning electron microscope. The AFM system is based on a home-built mechanical setup interfaced with controllers SPM1000 and PLLPro2 from RHK Technology.

We investigated two types of samples: S1 having 240 nm thickness (Figs. 2(a) and 3(a)) and S2 having 60 nm thickness (Figs. 2(b) and 3(b)).

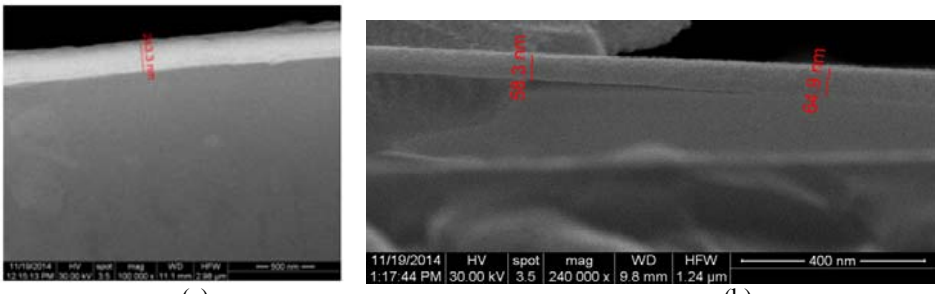

(a) (b)

Figs. 2 a), b). The SEM images of S1 having 240 nm thickness (a), and S2 having 60 nm thickness (b).

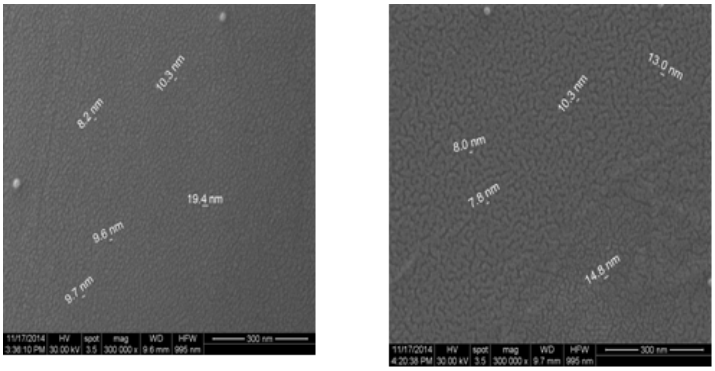

(a) (b)

Fig. 3 a), b). Surface images of S1 having 240 nm thickness (a), and S2 having 60 nm thickness (b).

In Fig. 2 we present the SEM images of the As_2S_3 nanostructured thin films deposited on glass. These secondary electrons images obtained with magnification 100000x indicate a high homogeneity and continuity of the films. One can observe a good adherence of the A_2S_3 thin film on the glass surface

because there are no holes between the glass substrate and the A_2S_3 thin film. Also, from Fig. 2 one can observe the uniformity of the thin film thickness along great dimensions in several zones, from both probes. From the Fig.3, the surface characteristics are emphasized as uniform nanograins in several zones, from both probes.

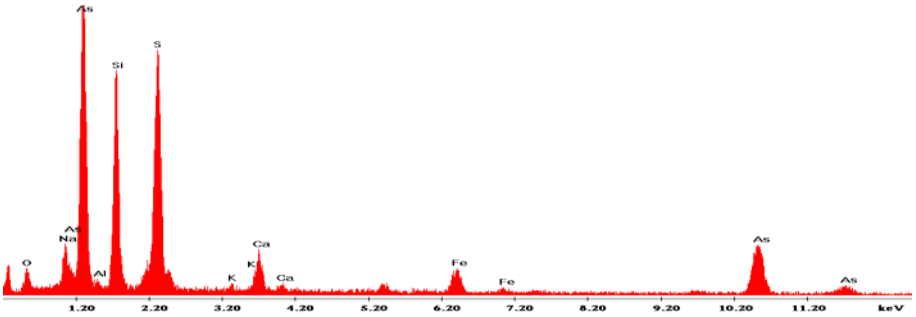

Fig. 4. The energy dispersive X-ray spectra of the As_2S_3 thin film on the Au layer chipset using glass substrate.

Energy dispersive X-ray microanalysis (EDAX) was performed in order to obtain the chemical local composition of the samples. The spectrum presented in Fig. 4 shows the presence in the thin film of the As, S on Au substrate. Due to the small thickness of the thin film (smaller than 1 μm) one remarked the presence of the elements which compose the glass substrate in S1 sample (Fig. 4).

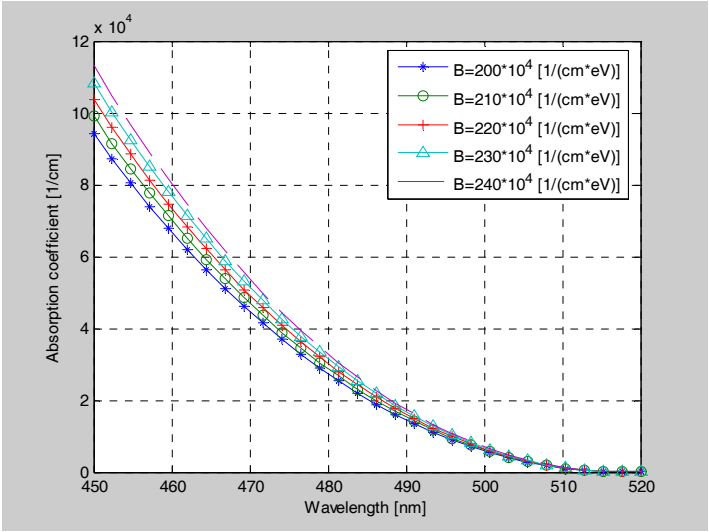

Fig. 5. The absorption coefficient of the amorphous As_2S_3 chalcogenide glasses vs wavelength, at different values of Tauc parameters.

Next, we evaluated the absorption coefficient of the amorphous As_2S_3 chalcogenide glasses in the spectral region 450-520 nm by using the Tauc model (Fig. 5), based on the theoretical models presented in Section 3 and considering $E_g \cong 2.39$ eV [14].

The value of the Tauc parameter B is situated in the range $200 \cdot 10^4 \div 240 \cdot 10^4$ for laser wavelengths between 450-520 nm which include the Ar^+ lasers (which are usually employed for analysing the optical properties of As_2S_3 chalcogenides) and the Thorlabs MCLS diode laser system (employed here for the experiments in Section 4).

Knowing the value of the absorption coefficient, determined experimentally or evaluated theoretically, one can evaluate the value of the optical band-gap energy E_g from the Tauc plot $(\alpha h\nu)^{1/2}$ vs the photon energy. Considering several values of the absorption coefficient of the amorphous As_2S_3 chalcogenide glasses calculated using the theoretical model presented in paper [14] we evaluated the optical band-gap energy Eg from the Tauc plot vs the photon energy, obtaining a value $E_g \cong 2.39$ eV (Fig. 6).

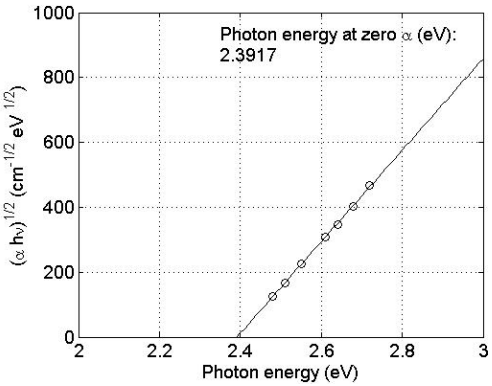

Fig. 6. The Tauc plot of the optical absorption coefficient $(\alpha h\nu)^{1/2}$ vs the photon energy. The solid curve represents a linear fitting curve of the data, extrapolated to zero

For several chalcogenide glasses the increase in E_c may be due to the quantum confinement effects that induce an increase in band gap, which may lead to an increase in the degree of tailing. A decrease (i. e. in the case of the Se sublayer thickness) results in a small increase in structural disorder connected with a possible bond angle distribution change [14]. A decrease in Urbach energy E_c is observed after photodiffusion. During photodiffusion the density of bonds (i. e. the case Se–Se) decreases and changes in conduction and valence band states may occur [14].

The above evaluated constants, Tauc parameter, B and Urbach energy, E_g may be used for the fabrication of the amorphous As_2S_3 chalcogenide film glasses and also for the better understanding of the absorption mechanisms in these structures.

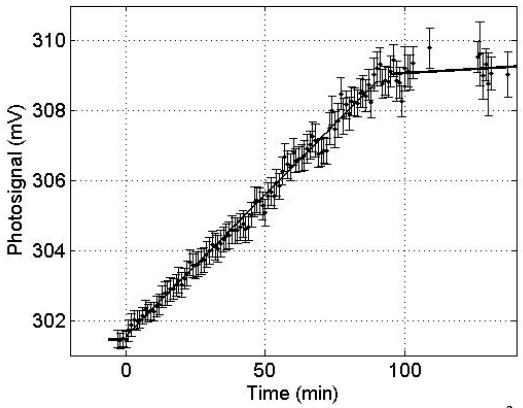

Fig. 7. Time dependence of the average photosignal for ~100 mW/cm^2 pump power. Time zero corresponds to the initiation of pump irradiation

We further investigated the optical properties of the As_2S_3 thin films by determining the photoinduced birefringence of the chalcogenic films. Under the experimental conditions presented in Section 4, during the first 90 minutes of irradiation we observed an approximate linear increase of the average photosignal displayed on the oscilloscope from 301 mV to about 309 mV (Fig. 7). At later times, a saturation of the photosignal is observed.

The photosignal variation between 301 mV and 309 mV indicates an approximate 2.5% increase of the film transmission. Apparently, the increase of film transmission is in contrast with the photo-darkening process which consists of increase losses of the chalcogenides under appropriate wavelength and pump intensity. The transmission increase during pump irradiation could be related to the small thickness of the chalcogenide film, to small absorption coefficient of the film at the pump wavelength (see Fig. 6), and to the interference phenomenon of the probe beam due to multiple reflections within the chalcogenide film. Thus, since the film thickness d is smaller than the probe beam wavelength λ, the intensity of the probe beam is strongly influenced by the constructive or destructive interference occurring due to multiple-reflections within the chalcogenide film. According to [15], the transmission of the optical structure consisting of the thin chalcogenide film deposited on the transparent substrate is

determined by the parameter δ which is dependent on the film refractive index n_f:

$$T = \frac{4n_f^2 n_s}{2n_f^2(n_s{}^2+1)+(n_f^2-1)(n_f^2-n_s^2)\sin^2(\delta)} \tag{4}$$

Here, $\delta = 2\pi n_f d/\lambda$, d=240nm, n_f=2.47 and n_s=1.51 is the refraction index of the substrate. Depending on the initial value of δ, i.e. on the initial value of n_f before the initiation of irradiation, the photo-induced variation of the refraction index could lead to the increase or to the decrease of the transmission during the pump irradiation. In our experimental conditions, the 2.5% increase of the film transmission during the first 90 minutes pump irradiation is determined by an approximate 0.02 variation of the refraction index.

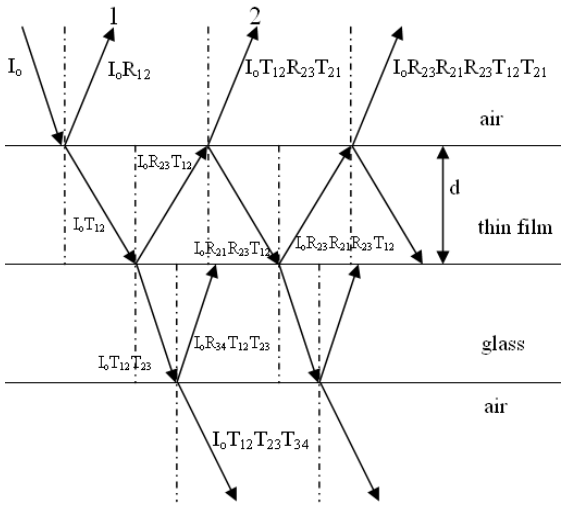

Fig. 8. The multiple reflections phenomenon on the air-film-glass-air structure [16].

Our samples consist in As_2S_3 thin film deposed on a glass substrate. When light hits a material that has multiple layers (in our case the air-film-glass-air structure), each layer can reflect the light (Fig. 8). The Fresnel equations provide a quantitative description of how much light will be reflected or transmitted at an interface. Further, interference processes occur at any interface in transmission and/or reflection. In our simulations the reflected intensity at air-film interface, considering the multiple reflections at all interfaces, was approximated by the relation:

$$I \cong R_{12} + T_{12}R_{23}T_{21} + 2\cdot\sqrt{R_{12}}\cdot\sqrt{T_{12}R_{23}T_{21}}\cos(2\delta), \tag{5}$$

where we considered the interference of only two rays (1 and 2 from Fig. 8). In relation (5) R_{ij}, with $i, j = 1,2,3,4$, represents the reflectance at ij interface, T_{ij} is the transmittance at ij interface and δ represents the optical path difference. The condition for interference is given by the value of the optical path difference. In the case of the As_2S_3 thin film, it is given by:

$$\delta = \frac{2\pi}{\lambda} n_f d \cos(\theta_2) \tag{6}$$

where λ is the wavelength (in our simulations $\lambda = 520\,nm$), $n_f = 2.47$ represents the refractive index of As_2S_3 thin film, $d = 240\,nm$ is the film thickness and θ_2 represents the refraction angle at air-film interface.

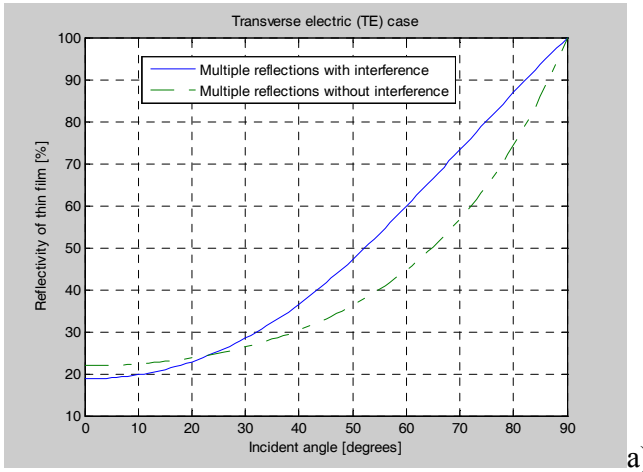

a)

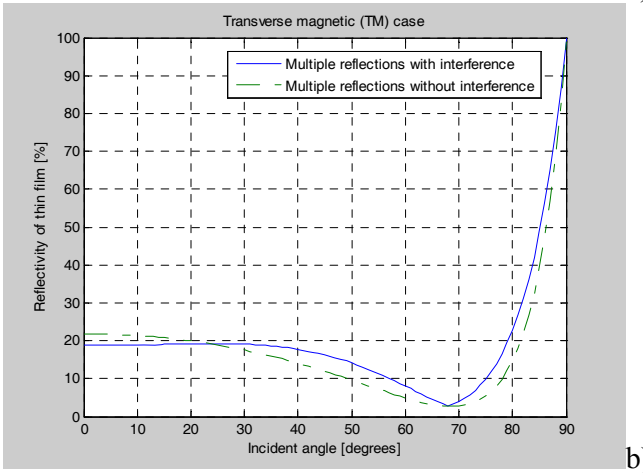

b)

Figs.9 a), b). The reflectance variation for TE and TM polarized waves versus the incidence angle, considering the multiple reflections phenomenon with and without interference.

By means of Fresnel relations we obtained the reflectance and transmittance of the s (transverse electric (TE)) and p (transverse-magnetic (TM)) polarized waves. In Figs. 9 a) and b) are presented the results of the reflectance variation of As_2S_3 thin film depending on the incidence angle for both s and p polarizations (TE and TM cases), considering the multiple reflections phenomenon with and without interference phenomenon.

The Fig. 10 shows that these two cases (multiple reflections with and without interference) have opposite effects on the reflectance of the As_2S_3 thin film. Thus, at a 0.01 variation of thin film refractive index ($n_f = 2.47 \div 2.48$), the effect of multiple reflections with interference leads to an approximate 4% decrease of thin film reflectance, and in the case of multiple reflections without interference occurs an increase of thin film reflectance (of about 0.8%). The cumulative effect of the two phenomena leads to an approximate 3.2% decrease of As_2S_3 thin film reflectance, which signifies an increase of thin film transmittance, according to the experimental results.

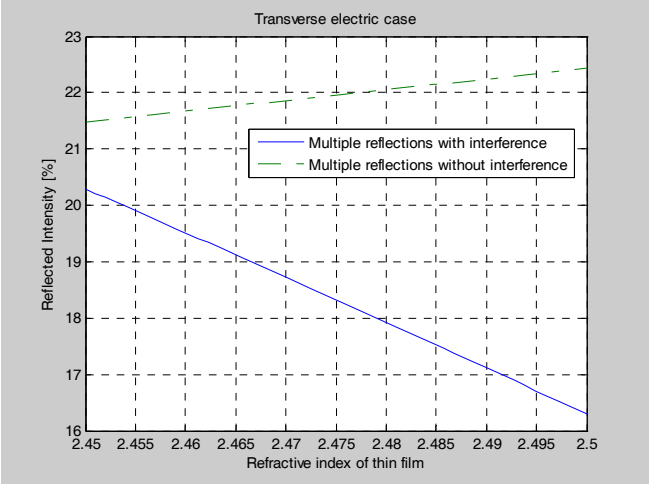

Figs.10. The reflectance variation for TE polarized waves versus the refractive index of As_2S_3 thin film, considering the multiple reflections phenomenon, with and without interference.

6. Conclusions

In the present article we report several theoretical and experimental results concerning the characterization of As_2S_3 film chalcogenide glasses by photoinduced optical absorption. We evaluated the absorption coefficient of the chalcogenide glasses using Tauc model in the range 450 nm÷510 nm range and the Urbach energy.

The photo-induced birefringence of the chalcogenic film was analysed experimentally. At intensities of the order of 100 mW/cm^2 of the pump laser, the transmission of the probe beam increases approximately linearly during the first 90 minutes and saturates at laser times. This was connected to the small film absorption at the pump wavelength, as demonstrated by the Tauc plot method, and to the destructive interference of the probe beam by multiple reflections within the chalcogenic film which enhances the film transmission during the pump irradiation.

The above mentioned theoretical and experimental results may be used for the fabrication of the amorphous As_2S_3 chalcogenide film glasses and also for the better understanding of the absorption mechanisms in these structures.

Acknowledgements

This work was supported by the Romanian National Authority for Scientific Research, CNDI – UEFISCDI, through grant PN-II-PT-PCCA-2011-25/2012.

R E F E R E N C E S

[1] *Kretschmann, E. and Raether, H.* (1968). Radiative decay of non-radiative surface plasmons excited by light. Z. Naturforschung, 23A: 2135-2136

[2] *A. Otto*, Excitation of nonradiative surface plasma waves in silver by the method of frustrated total reflection, Zeitschrift für Physik A Hadrons and Nuclei, Vol. **216**, No. 4, p. 398–410, (1968).

[3] *S. A. Maier*, Plasmonics – Fundamentals and Applications, Springer, New York, (2007).

[4] *Georgiana C. Vasile, A. A. Popescu, M. Stafe, S. A. Koziukhin, D. Savastru, Simona Donțu, L. Baschir, V. Sava, B. Chiricuță, M. Mihăilescu, C. Neguțu, N. N. Puşcaş*, Plasmonic waveguides features correlated with surface plasmon resonance performed with a low refractive index prism, University "Politehnica" of Bucharest, Scientific Bulletin, Series A: Applied Mathematics and Physics, Vol. **75**, No. 4, p. 311-325, 2013.

[5] A. *Moldovan, M. Enăchescu, A. A. Popescu, M. Mihăilescu, C. Neguțu, L. Baschir, G. C. Vasile, D. Savastru, M. S. Iovu, V. I. Verlan, O. T. Bordian, I. M. Vasile, N.N. Puşcaş*, Characterization of As2S3 thin surface films using SEM and AFM methods, University "Politehnica" of Bucharest, Scientific Bulletin, Series A: Applied Mathematics and Physics, Vol. **76**, No. 2, p. 215-222, (2014).

[6] *A. A. Popescu, M. Mihăilescu, C. Neguțu, L. Baschir, M. Stafe, G. C. Vasile, D. Savastru, M. S. Iovu, V.I. Verlan, O. T. Bordian, A. Moldovan, M. Enăchescu, N. N. Puşcaş*, Preparation of chalcogenide bulk and thin films and their characterization using optical methods, University "Politehnica" of Bucharest, Scientific Bulletin, Series A: Applied Mathematics and Physics, Vol. **76**, No. 3, p. 211-218, (2014).

[7] *Z. Opilski*, Analysis of Surface Plasmons in a Planar Waveguide System with Spectral Detection — Results of Model Investigations, Acta Phys. Pol. A, Vol. **118**, No. 6, p. 1215-1220, (2010).

[8] *I. Abdulhalim, M. Gelbaor, M. Klebanov, and V. Lyubin*, Photoinduced phenomena in nano-dimensional glassy As_2S_3 films, Optical Materials Express, Vol. **1**, No. 7, 1192-1201, (2011).

[9] *M. S. Iovu, I. A. Cojocaru, E. P. Colomeico,* Photoinduced phenomena in α-As2S3 films doped with Pr3+, Dy3+ AND Nd3, Chalcogenide Letters, Vol. **4**, No. 5, p. 55-60, (2007).
[10] *A. R. Zanatta and I. Chambouleyron,* Absorption edge, band tails, and disorder of amorphous semiconductors, Phys. Rev. B, Vol. **53**, p. 3833-3839, p. (1996)
[11] *F. Urbach,* The long-wavelength edge of photographic sensitivity and of the electronicabsorption of solids, Physical Review, Vol. **92**, No. 5, p. 1324-1953, (1953).
[12] *P O'connor, J Tauc,* Photoinduced midgap absorption in tetrahedrally bonded amorphous semiconductors, Phys. Rev. B, Vol. 4, p. 2748-2756, (1982)
[13] *N. F. Mott and E. A. Davis,* Electronic Process in Non-crystalline Materials, Clarendon, Oxford, (1979)
[14] *K. V. Adarsh, K. S. Sangunni, T. Shripathi, S. Kokenyesi, and M. Shipljak*, Photoinduced interdiffusion in nanolayered Se/As2S3 films: Optical and x-ray photoelectron spectroscopic studies, J. Appl. Phys. Vol. 99, p. 094301-6, (2006).
[15] *A. A. Popescu, D. Savastru, S. Miclos*, Refractive index anisotropy in non-crystalline As_2S_3 films, J. Optoelectron. Adv. M., Vol. 12(5), p. 1012-1018, (2010).
[16] *H. Hauss*, Waves and Fields in Optoelectronics, Prentice-Hall, Inc. Englewood Cliffs, (1984).